Communications Research Centre

A SPECTROSCOPIC DETERMINATION OF THE INDUCED-EMISSION CROSS SECTION OF THE $^3P_0 \rightarrow\!\!\rightarrow {}^3F_2$ AND $^3P_0 \rightarrow\!\!\rightarrow {}^3H_6$ TRANSITIONS OF THE Pr^{3+} ION IN $SeOCl_2 : SnCl_4$

by

A. Watanabe

CRC REPORT NO. 1243

DEPARTMENT OF COMMUNICATIONS
MINISTÈRE DES COMMUNICATION

OTTAWA, JULY 1973

COMMUNICATIONS RESEARCH CENTRE

DEPARTMENT OF COMMUNICATIONS
CANADA

A SPECTROSCOPIC DETERMINATION OF THE INDUCED-EMISSION CROSS SECTION OF THE $^3P_0 \rightarrow\rightarrow {}^3F_2$ AND $^3P_0 \rightarrow\rightarrow {}^3H_6$ TRANSITIONS OF THE Pr^{3+} ION IN $SeOCl_2$:$SnCl_4$

by

A. Watanabe

(Informatique Directorate)

CRC REPORT NO. 1243

July 1973

OTTAWA

TABLE OF CONTENTS

A SPECTROSCOPIC DETERMINATION OF THE INDUCED-EMISSION CROSS SECTION OF THE $^3P_0 \rightarrow\!\!\rightarrow {}^3F_2$ AND $^3P_0 \rightarrow\!\!\rightarrow {}^3H_6$ TRANSITIONS OF THE Pr^{3+} ION IN $SeOC\ell_2 : SnC\ell_4$

by

A. Watanabe

ABSTRACT

We have used a spectroscopic method to determine the induced-emission cross-section for the $^3P_0 \rightarrow\!\!\rightarrow {}^3F_2$ and $^3P_0 \rightarrow\!\!\rightarrow {}^3H_6$ transitions of the Pr^{3+} ions in an aprotic solvent system consisting of a 4: mixture of $SeOC\ell_2$ and $SnC\ell_4$. The values obtained were $4.3 \times 10^{-19} cm^2$ and $2.0 \times 10^{-19} cm^2$, respectively. The former value is five times as large as the value $0.85 \times 10^{-19} cm^2$ for the low-theshold laser transition of the Nd^{3+} ion in the same solvent system, so that this system warrants further study as a laser material.

1. INTRODUCTION

The spectroscopy of rare-earth ions has proved, in the past, to be a fruitful area of research; the spectra of Nd^{3+} and Eu^{3+} ions, in particular, have been studied in crystals, glasses and chelates and aprotic solvents and many of these rare-earth-doped system have been shown to have excellent characteristics as laser materials[1-8]. We have carried out a spectroscopic study of Pr^{3+} ions in $SeOC\ell_2$-based solvent systems and have previously reported evidence for a local field of D_{2d} symmetry about the rare-earth ion[9].

In the study of any laser system one of the most important criteria is the start oscillation condition, or the critical population inversion at the threshold of laser oscillation. This critical condition can be related simply to parameters characterizing the laser resonator and the lasing medium, namely, the length of the resonator, resonator losses and the induced-emission cross section of the laser transition[10]. Thus a measure of the induced-emission

cross section is of importance in the study of any laser system. In the present report we describe a spectroscopic determination of the induced-emission cross section of two potential laser transitions of the Pr^{3+} ion in $SeOCl_2$:$SnCl_4$. We have obtained values of the induced-emission cross section for the $^3P_0 \rightarrow\rightarrow {}^3F_2$ and $^3P_0 \rightarrow\rightarrow {}^3H_6$ transitions of the Pr^{3+} ion in the liquid solvent consisting of a mixture of $SeOCl_2$ and $SnCl_4$. The values obtained were 4.3×10^{-19} cm^2 and 2.0×10^{-19} cm^2, respectively, for the two transitions. These values compare favourably with the value 0.85×10^{-19} cm^2 for the laser transition of the Nd^{3+} ion in the same solvent[11], so that these transitions appear to be good candidates for laser action.

2. ABSORPTION CROSS SECTION AND RADIATIVE LIFETIME

According to Einstein's treatment of a quantized system of radiators, the probability than an atom in a state n will absorb a quantum of radiation of energy $h\nu_{nm}$ and undergo transition to a higher state m in unit time is given by

$$P_{nm} = B_{nm}\rho(\nu_{nm}), \qquad .....(1)$$

where B_{nm} is called Einstein's coefficient of absorption and $\rho(\nu_{nm})$ is the density of radiation at frequency ν_{nm}. The probability that the atom in state m will in unit time emit a quantum of radiation of energy $h\nu_{mn}$ and pass to the lower state n is given by

$$P_{mn} = A_{mn} + B_{mn}\rho(\nu_{mn}), \qquad .....(2)$$

where A_{mn} is Einstein's coefficient of spontaneous emission and B_{mn} is Einstein's coefficient of induced emission. If the upper state is g_m-fold degenerate and the lower state is g_n-fold degenerate, then the following relations hold between the coefficients:

$$g_n B_{nm} = g_m B_{mn}, \qquad .....(3)$$

and

$$A_{mn} = \frac{8\pi h\nu_{mn}^3 B_{mn}}{c^3}, \qquad .....(4)$$

where h is Planck's constant and c is the velocity of light.

If the state n is the ground state or a low lying level, it is thermally populated at normal temperatures and conventional absorption spectroscopy can be used to determine B_{nm}, and the other two coefficients can be calculated from it by the use of equations (3) and (4) above. In most 4-level laser systems, level n is usually completely depopulated at normal temperatures and other methods must be used to measure these coefficients. One method of determining B_{nm} is from the fluorescence changes of an excited medium caused

by a resonance laser pulse[12]. Another method is based on the measurement of the change in the gain coefficient of a laser associated with the change in the energy stored in the cavity[13,14]. Pantoflicek[15] has reported a purely spectroscopic method based on the relationship between the oscillator strength and the absorption cross section.

In this report we follow a spectroscopic method first used by Neeland and Evtuhov[16] for the measurement of the laser transition cross section for Nd^{3+} ions in yttrium aluminum garnet (YAG). The method does not depend on the determination of a quantum yield or on any assumptions dependent on such a determination. It consists essentially of measuring B_{nm} for a ground state transition, and then measuring the ratios of A_{mn} for several fluorescence transitions, including the transition to the ground state, for which B_{nm} was measured. Thus all of the other coefficients can be deduced with the aid of equations (3) and (4) above. The absorption coefficient can be expressed in various ways; for example, it can be expressed as an absorption cross section per molecule, σ_{nm}. On the other hand the measured coefficient is most easily expressed as an absorption coefficient per unit path length through the sample, $k(\nu)$. The absorption cross section is usually referred to the peak value, $k(\nu_0)$, of the absorption coefficient at a frequency ν_0. Thus

$$\sigma_{nm} = \frac{k_{nm}(\nu_0)}{N_n} , \qquad .....(5)$$

where N_n is the number of active molecules per volume of sample.

From equation (2) it is clear that the probability that an atom in state m will in unit time spontaneously emit a quantum of radiation and pass to the lower state n is given by A_{mn}. Thus we write

$$A_{mn} = \frac{1}{\tau_{mn}} , \qquad .....(6)$$

where τ_{mn} is the radiative lifetime of the transition from m to n. With the aid of equations (3), (4) and (6), it can be shown[17] that the integrated absorption coefficient of an absorption line α_{nm} is related to the radiative lifetime of the transition by the following expression:

$$\alpha_{nm} = \int_0^\infty k_{nm}(\nu)d\nu = \frac{\lambda^2}{8\pi}\frac{g_m}{g_n}\frac{N_n}{\tau_{mn}} , \qquad .....(7)$$

where λ is the value of the wavelength in the medium at the peak value of the absorption coefficient. This expression can be used to calculate the radiative lifetime of a transition from the measured integrated absorption coefficient.

When the shape of the absorption line is defined by the equation

$$k_{nm}(\nu) = k_{nm}(\nu_0) \frac{f_{nm}(\nu)}{f_{nm}(\nu_0)} , \qquad .....(8)$$

where $f_{nm}(\nu)$ is a line shape function defined such that $\int_0^\infty f_{nm}(\nu)d\nu = 1$, then

$$\alpha_{nm} = \frac{k_{nm}(\nu_0)}{f_{nm}(\nu_0)} . \qquad .....(9)$$

The reciprocal of $f_{mn}(\nu_0)$ plays the role of an effective halfwidth of the line. If the line-shape function is triangular for a line of halfwidth δ, then

$$f_{mn}(\nu_0) = \frac{1}{\delta} . \qquad .....(10)$$

If the line shape is lorentzian, then

$$f_{mn}(\nu_0) = \frac{2}{\pi\delta} , \qquad .....(11)$$

For a gaussian line shape

$$f_{mn}(\nu_0) = \frac{2(\ell n2)^{\frac{1}{2}}}{\pi^{\frac{1}{2}}\delta} . \qquad .....(12)$$

When the line-shape function is not known exactly, numerical value for $f_{mn}(\nu_0)$ can be derived from the experimental data, since it is expressed in equation (9) as the ratio of the peak height to the integrated area of the fluorescence (or absorption) line for the mn transition. Neeland and Evtuhov[16] assumed a triangular line-shape function in their determination.

If the line shape is the same for the nm and mn transitions, equation (3) can be written as

$$g_m\sigma_{mn} = g_n\sigma_{nm}, \qquad .....(13)$$

where σ_{mn} is the induced-emission cross section. Thus equation (7) becomes

$$\sigma_{mn} = \frac{\lambda^2 f_{mn}(\nu_0)}{8\pi\tau_{mn}} . \qquad .....(14)$$

This equation can be used to determine the induced-emission cross section when the radiative lifetime of the transition is known.

3. MEASUREMENT OF THE INDUCED-EMISSION CROSS SECTION

The solutions were prepared from dried praseodymium chloride[18] and vacuum-distilled liquids[19], following the detailed preparative techniques described by Heller[20]. Sample preparation procedures were carried out in a nitrogen atmosphere inside an evacuable stainless-steel glove box[21]. The moisture level within the box was maintained at less than 10 ppm by volume, and the moisture content of the prepared samples was determined by infrared absorption measurements to be less than 1 part in 10^7.

The solvent consisted of $SeOC\ell_2$ and $SnC\ell_4$ in a ratio of 4 to 1. Preliminary experiments with samples of Pr^{3+} in the range 3×10^{-3} N to 3 N showed that a rare-earth concentration of 0.1 N gave a good compromise between fluorescence intensity and quenching effects, and subsequent measurements were carried out on samples of this concentration. The fluorescence cells were made from lengths of thick-wall quartz capillary tubing of i.d. 2 mm which were stoppered at both ends by teflon plugs; this construction facilitated the drying out of the cell. The absorption cells were commercials cells of thickness 2 cm.

Absorption spectra were measured on a Cary 14 spectrophotometer. The fluorescence spectra were recorded on a fluorescence spectrometer that was constructed in our laboratory. The essential parts of the spectrometer are shown schematically in Figure 1. The source of radiation was a 1000-watt xenon arc lamp in a commercial housing. A circulating water filter removed infrared radiation from the light beam before it was focused on the entrance slit of a ¼ m Ebert grating monochromator. The wavelength of the excitation light was controlled by means of this monochromator working in conjunction with auxiliary optical band-pass filters. The fluorescence emission from the samples was optically chopped and then focused on the slit of a 1 m Czerny-Turner grating monochromator, where it was dispersed with a grating with 1800 lines/mm. The dispersed light was detected with an ITT FW-130 photomultiplier with a slit-shaped cathode. The signal from the photomultiplier was rectified and smoothed in a Princeton Applied Research HR-8 lock-in amplifier and recorded on a strip-chart recorder. The optical response of the fluorescence spectrometer was calibrated with the aid of an Electro-Optic Associates L-101 Spectral Irradiance Standard.

In the rare-earth ions, such as Pr^{3+}, the partially filled 4f-electron shell lies within some of the completely filled shells; thus the interaction of the 4f electrons with the external environment is weak, and the free-ion energy levels[22] give a good representation of the energy levels in bulk media. These energy levels are shown in Figure 2.

The Pr^{3+} ion has three strong absorption lines in the region 0.450 - 0.500 μm (see Figure 3), which arise from transitions from the ground state, $^3H_4$, to the triplet states $^3P_{0,1,2}$. The ^3P states are close together and internal coupling leaves the ion in the lowest state $^3P_0$. The fluorescence spectrum (Figure 4) has four strong lines, at 0.484, 0.597, 0.613 and 0.642 μm. The first is the resonance transition from $^3P_0$ to the ground state, and the last two were identified from their energy, their excitation spectra and the time decay of the fluorescence radiation under pulsed excitation, as transitions from $^3P_0$ to $^3F_2$ and $^3H_6$, respectively. The line at 0.597 μm appears to be a transition from the $^1D_2$ to the $^3H_4$ state.

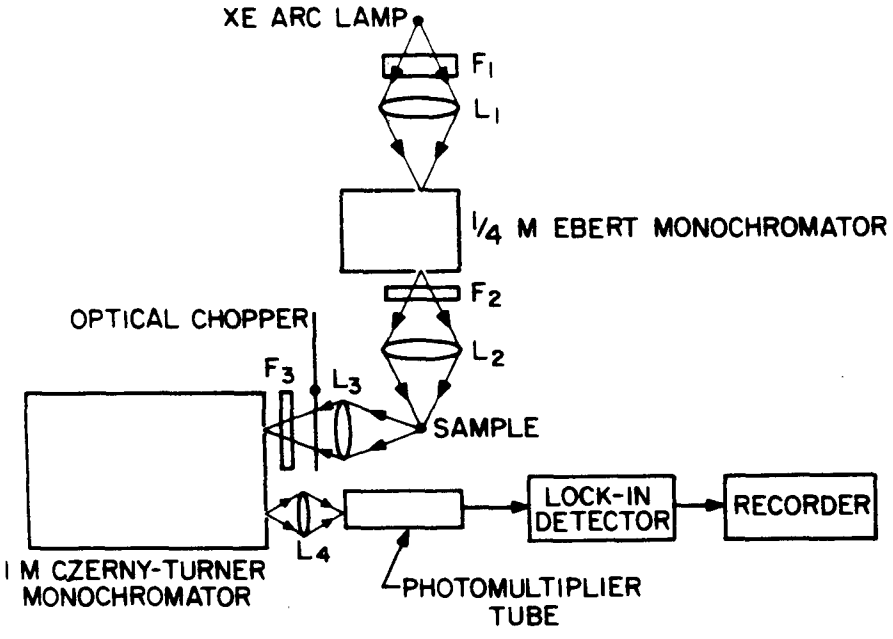

Fig. 1. A schematic diagram of the fluorescence spectrometer showing its essential parts. L_1, L_2, L_3 and L_4 are lenses and F_1, F_2 and F_3 are optical filters. The optical path is indicated by the faint lines.

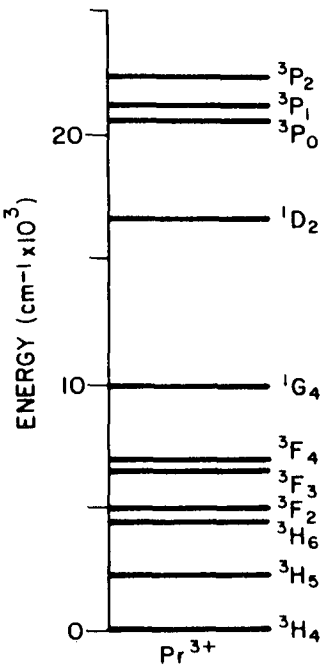

Fig. 2. The free-ion energy levels of the Pr^{3+} ion.

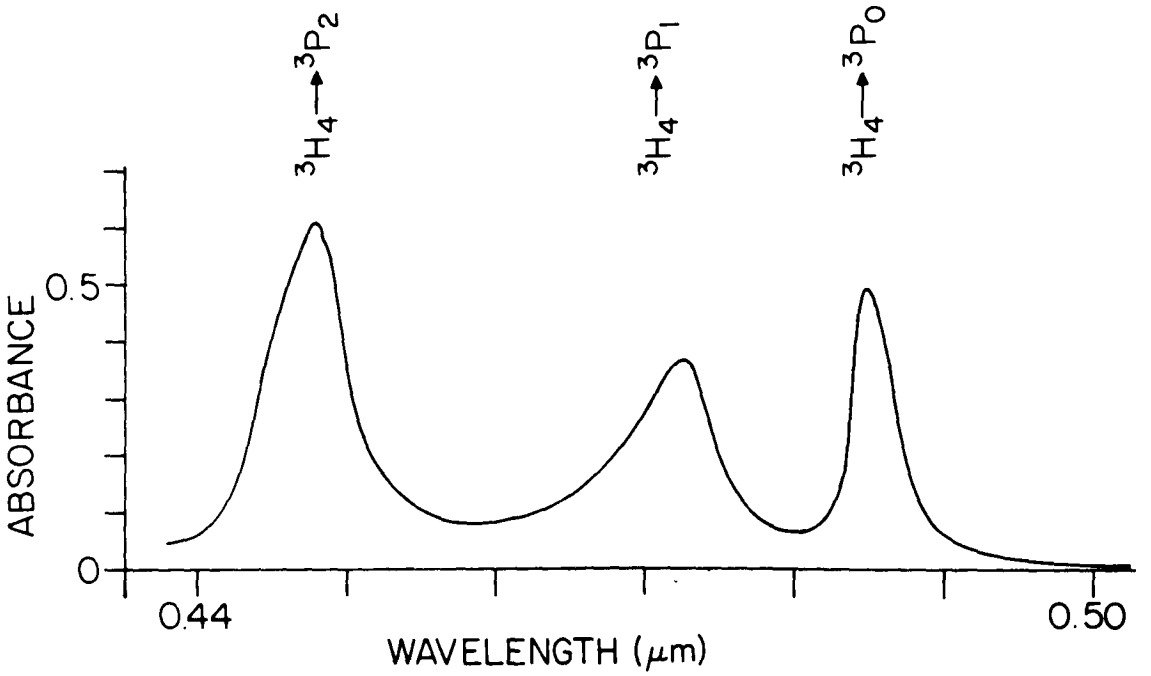

Fig. 3. A portion of the absorption spectrum of Pr^{3+} in $SeOCl_2$:$SnCl_4$ for a 0.1 N sample in a 20 mm absorption cell.

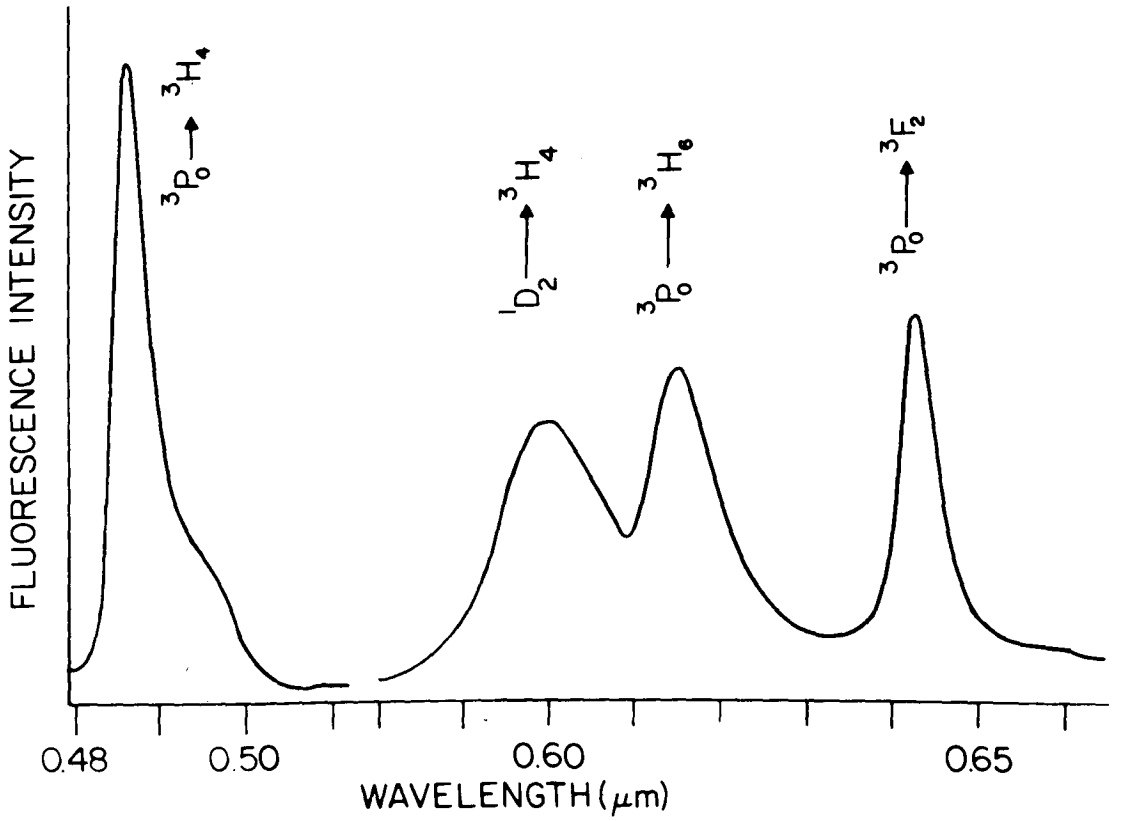

Fig. 4. A portion of the fluorescence spectrum of Pr^{3+} in $SeOCl_2$:$SnCl_4$.

The induced-emission cross section was measured for the 0.613 and 0.642 μm transitions. Since the terminal levels for both transitions lie well above the ground state, a direct measurement of the absorption coefficient was not possible. Therefore the value was obtained indirectly from a measurement of the cross section for the transition from the ground state $^3H_4$ to $^3P_0$, following the method reported by Neeland and Evtuhov[16]. For convenience we label the $^3H_4$, $^3H_6$, $^3F_2$ and $^3P_0$ manifolds by the quantum number n = 1, 2, 3 and 4, respectively. The method consists of the following steps: σ_{14} is measured from the absorption spectra and σ_{41} and τ_{41} are calculated from it by the use of equations (3) and (7); then τ_{42} and τ_{43} are calculated from τ_{41} and the measured fluorescence intensity ratios; finally σ_{42} and σ_{43} are calculated from τ_{42} and τ_{43} with the aid of equation (14).

Since the $^3P_0$ state is non-degenerate and the $^3H_4$ state is 9-fold degenerate, the transition can consist of up to nine components. In a previous paper we showed that the Pr^{3+} ions occupy sites of D_{2d} symmetry and that only electric-dipole transitions are required to account for the features of the fluorescence spectra. A computer analysis of the $^3P_0 \rightarrow\rightarrow {}^3H_4$ fluorescence band[9] showed that it could be reproduced quite accurately by the summation of three gaussian components, whose separation, peak intensities, half-widths, and relative areas are given in Table 1. In calculating the value of the absorption cross section we must know the value of the population of each of the levels, since the value is required of the partition function of the ground state

$$Q = \sum_i g_i \exp\left[-\Delta E_i/kT\right] \qquad .....(15)$$

where g_i and ΔE_i are the degeneracy and the energy displacement of the i^{th} component of the ground state, respectively, k is Boltzmann's constant, and T is the absolute temperature. The observed transitions terminate in two doubly-degenerate levels and a non-degenerate level (see Figure 5). A very weak feature observed at an energy displacement of approximately 1000 cm^{-1} could arise from a transition terminating in one of these single levels. Another of the non-degenerate levels should lie reasonably close to the doubly-degenerate level at 333 cm^{-1}, as these levels have common parentage in the level of T_1 symmetry in the cubic field approximation. The location is not known of the remaining two non-degenerate levels, which are derived from the level of E symmetry in the cubic field approximation. From the calculations of Lea, Leask and Wolf[23] of the splittings of the energy levels of rare-earth ions in cubic fields, we calculate the value of the partition function Q as a function of the crystal-field parameter x. We have made use of the observed splitting of approximately 333 cm^{-1} between the T_2 and T_1 levels to scale the energy values. A plot of Q versus x is shown in Figure 6 for the $^3H_4$ level for the possible range of values of x for which the T_2 level is lowest lying. For the purposes of our present determination we use the average value of the maximum and minimum values, and take Q = 4.45 ± 0.26.

TABLE 1

The Gaussian Components of the $^3P_0 \rightarrow\rightarrow ^3H_4$ Fluorescence Band

Energy Separation (cm^{-1})	Half-Width (cm^{-1})	Peak Intensity (arbitrary units)	Area (arbitrary units)
0	73.5	0.491	0.300
66	144	0.371	0.444
333	223	0.138	0.256

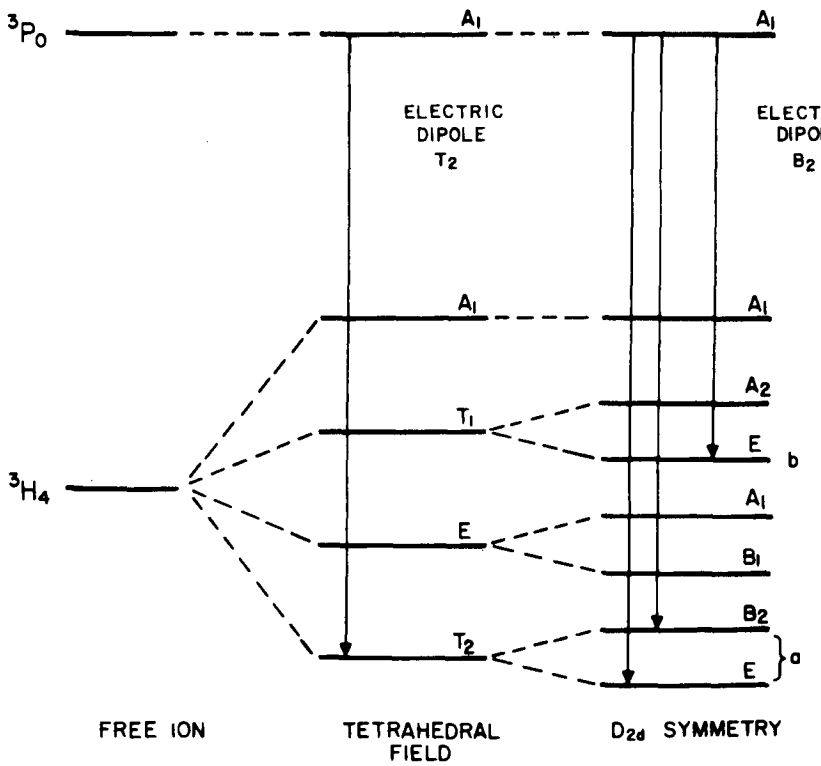

Fig. 5. The electric-dipolar allowed transitions between the $^3P_0$ and $^3H_4$ states of the Pr^{3+} ion in a tetrahedral field and in a field of D_{2d} symmetry.

It is apparent from the analysis of the $^3H_4$ manifold that the doublet and singlet levels which originate in the T_2 level of the cubic field together account for more than 99 per cent of the observed absorption at the peak of the absorption line. Since we can readily separate out the contribution to the induced emission of these two levels from the contribution of the third active level, which is split $333 cm^{-1}$ from the ground state, we treat the two lowest levels as the ground state. We label this state by the letter a and the other active level by b, as shown in Figure 5. Therefore

$$\sigma_{41} = \sigma_{4a} + \sigma_{4b} \cdot \qquad \ldots\ldots(16)$$

Since level a is thermally populated we can determine σ_{4a} by the method outlined above and subsequently σ_{4b} can be determined by making use of the analysis of the fluorescence band shape for the 41 transition.

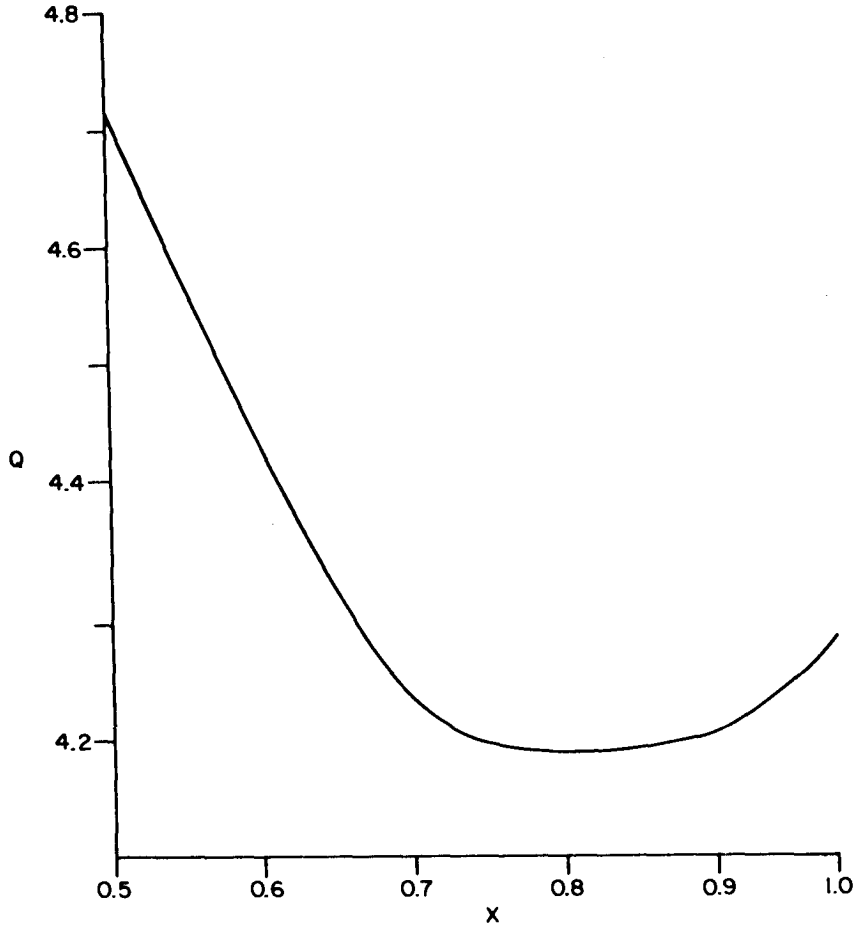

Fig. 6. The value of the partition function for the Pr^{3+} ion in a tetrahedral field plotted against the crystal field parameter x over all its possible values in a in a tetrahedral field for which the T_2 level is the lowest lying level.

The concentration of Pr^{3+} ions in the samples used in our determination was 0.1 N, so that the number of ions per volume is $N_0 = 2.01 \times 10^{19}$ ions/cm^2. Therefore the population of level a is given by

$$N_a = \frac{N_0}{Q} \sum_{i=a} g_i \, e^{-\Delta E_i/kT} = \frac{2.01 \times 10^{14}}{4.45} (2 + 0.724) = 1.23 \times 10^{19} \text{ ions/cm}^3.$$

The measured value of the absorption coefficient at the peak was

$$k_0 = 0.808 \text{ cm}^{-1}.$$

Therefore

$$\sigma_{a4} = \frac{k_0}{N_a} = \frac{0.808}{1.23 \times 10^{19}} \text{ cm}^2 = 6.57 \times 10^{-20} \text{ cm}^2,$$

$$\sigma_{4a} = \frac{g_a}{g_4} \sigma_{a4} = \frac{3}{1} \times 6.57 \times 10^{-20} \text{cm}^2 = 1.97 \times 10^{-19} \text{ cm}^2,$$

and

$$\sigma_{41} = \frac{1.000}{0.744} \times \sigma_{4a} = 2.65 \times 10^{-19} \text{ cm}^2.$$

By substituting measured values of the integrated area and the peak height of the fluorescence spectrum of the $^3P_0 \rightarrow\rightarrow {}^3H_4$ transition in equation (9) we obtain

$$\left[f_{41}(\nu_0)\right]^{-1} = 262 \text{ cm}^{-1}.$$

Thus from equation (14) we obtain

$$\tau_{41} = \frac{\lambda^2 f_{41}(\nu_0)}{8\pi \sigma_{41}} = \frac{(0.484 \times 10^{-4})^2}{8 \times 2.65 \times 10^{-19} \times 262 \times 3 \times 10^{10}} \text{ sec}$$

$$= 44.7 \text{ μsec}.$$

From equation (4) it is clear that

$$A_{43}\tau_{43} = A_{41}\tau_{41}, \qquad \text{.....(17)}$$

thus

$$\tau_{43} = \frac{A_{41}}{A_{43}} \tau_{41} = R_{43}^{41} \tau_{41}, \qquad \text{.....(18)}$$

where

$$R_{43}^{41} = \frac{A_{41}}{A_{43}}, \qquad \text{.....(19)}$$

is the ratio of the number of photons emitted in the 41 and 43 transitions. Similarly

$$\tau_{42} = R_{42}^{41}\tau_{42}, \qquad \text{.....(20)}$$

where R_{42}^{41} is the ratio of the number of photons emitted in the 41 and 42 transitions. The experimental values of R_{4n}^{41} and $f_{4n}(\nu_0)$ given in Table 2 were substituted in equations (18), (20) and (14) to obtain the following values:

$$\tau_{42} = 2.46 \times 44.7 \text{ μsec} = 109 \text{ μsec},$$

$$\tau_{43} = 1.81 \times 44.7 \text{ μsec} = 80.9 \text{ μsec},$$

$$\sigma_{42} = \frac{(0.613 \times 10^{-4})^2}{8\pi \times 109 \times 10^{-6} \times 225 \times 3 \times 10^{10}} \text{ cm}^2 = 2.03 \times 10^{-19} \text{ cm}^2,$$

$$\sigma_{43} = \frac{(0.642 \times 10^{-4})^2}{8\pi \times 80.9 \times 10^{-6} \times 157 \times 3 \times 10^{10}} \text{ cm}^2 = 4.30 \times 10^{-19} \text{ cm}^2.$$

These values are also listed in Table 2.

TABLE 2

Values for the Induced-Emission Cross Section and Related Parameters for Three Transitions of the Pr^{3+} ion in $SeOC\ell_2$:$SnC\ell_4$

Transition	$^3P_0 \rightarrow\rightarrow {}^3H_4$	$^3P_0 \rightarrow\rightarrow {}^3H_6$	$^3P_0 \rightarrow\rightarrow {}^3F_2$
λ (μm)	0.484	0.613	0.642
$\frac{1}{f(\nu_0)}$ (cm^1)	262	225	157
R_{4n}^{41}	1.00	2.46	1.80
τ_{4n}(μsec)	44.7	109	81
σ_{4n}(cm^2)	2.65×10^{-19}	2.0×10^{-19}	4.3×10^{-19}

4. DISCUSSION

When the crystal-filled splittings of the upper and lower manifolds are known, as is the case in many crystals, the method of Neeland and Evtuhov[16] for the determination of induced-emission cross sections is reasonably straightforward and can lead to accurate values. On the other hand, when the splittings are not clearly resolved, then the method can be less accurate, since the value of the partition function is required for the determination. The method may also have certain drawbacks in its application to ions with an even number of f electrons, such as the Pr^{3+} ion, where certain transitions are forbidden by electric-dipole selection rules. In this case, the value of the partition function can again be in doubt. For the particular determination described in this note the value of the partition function is probably good to within ±5 per cent, since it was possible to clearly separate[9] the allowed transitions of the $^3P_0 \rightarrow\rightarrow {}^3H_4$ band by means of a computer analysis. In the previous application of this method for the determination of the induced-emission cross section of the $^4F_{\frac{3}{2}} \rightarrow\rightarrow {}^4I_{\frac{11}{2}}$ transition of the Nd^{3+} ion in $SeOC\ell_2$ Samelson *et al.*[11] found it necessary to employ a certain amount of guess-work, in determining the value of the partition function and also in trying to decide which part of the fluorescence band pertained to the particular transitions for which the absorption coefficient was measured. In our case the computer analysis of the

fluorescence band has eliminated the necessity for all such guess-work. Thus the probable error of the measured value of the induced-emission cross section is less than ±10 per cent.

This determination has indicated that the Pr^{3+} ion in $SeOCl_2$:$SnCl_4$ has a sufficiently high value for the induced-emission cross section to warrant further study as a possible candidate for laser action. Other factors such as the efficiency of optical pumping, the radiative efficiency of the upper level and the optical quality of the solution must also be determined before a final judgement can be made.

5. ACKNOWLEDGEMENT

The author thanks R.G. Lamont for providing excellent technical assistance throughout the course of the experiments.

6. REFERENCES

1. Dieke, G.H. *Spectra and energy levels of rare earth ions in crystals.* (Interscience Publishers, New York), 1968.

2. Levine, A.K. ed., *Lasers.* (Marcel Dekker, Inc., New York) Vol. 1, (1966) and Vol. 2 (1968).

3. Heller, A. *A high-gain room-temperature liquid laser: trivalent neodymium in selenium oxychloride.* Appl. Phys. Lett. 9, 106 (1966).

4. Lempicki, A. and A. Heller. *Characteristics of the Nd^{3+}: $SeOCl_2$ liquid laser.* Appl. Phys. Lett. 9, 108 (1966).

5. Schimitschek, E.J., Nehrich, R.B. and J.A. Trias. *Recirculating liquid laser.* Appl. Phys. Lett. 9, 103 (1966).

6. Schimitschek, E.J. *Laser emission of a neodymium salt dissolved in $POCl_3$,* J. Appl. Phys. 39, 6120 (1968).

7. Heller, A. *Liquid lasers - design of neodymium-based inorganic ionic systems.* J. Mol. Spectroscopy 28, 101 (1968).

8. Heller, A. *Liquid lasers - fluorescence, absorption and energy transfer of rare earth ion solutions in selenium oxychloride.* J. Mol. Spectroscopy 28, 208 (1968).

9. Watanabe, A. *Non-cubic local structure in a Pr^{3+}-doped $SeOCl_2$:$SnCl_4$ solution.* To be published in Can. Journal of Physics.

10. Schawlow, A.L. and C.H. Townes. *Infrared and optical masers.* Phys. Rev. 112, 1940 (1958).

11. Samelson, H., Heller, A. and C. Brecher. *Determination of the absorption cross section of the laser transitions of the Nd^{3+} ion in the Nd^{3+}:$SeOCl_2$ system.* J. Opt. Soc. Am. 58, 1054 (1968).

12. Belan, V.R., Grigoryants, V.V. and M.E. Zhabotinski. *Use of lasers in measurements of the stimulated emission cross section.* IEEE J. Quantum Electron. QE-3, 425 (1967).

13. Mauer, P. *Amplification coefficient of neodymium-doped glass at 1.06 microns.* Appl. Opt. 3, 433 (1964).

14. Edwards, J.G. *Measurement of the cross-section for stimulated emission in neodymium glass.* Nature 212, 752 (1966).

15. Pantoflicek, J. *Calculation of the amplification coefficient of stimulated emission from fluorescence measurements.* Czech. J. Phys. B 17, 27 (1967).

16. Neeland, J.K. and V. Evtuhov. *Measurement of the laser transition cross section for Nd^{3+} in yttrium aluminum garnet.* Phys. Rev. 156, 244 (1967).

17. Mitchell, A.C.G. and M.W. Zemansky. *Resonance radiation and excited atoms.* (Cambridge University Press, New York) 1961.

18. Johnson, K.E. and J.R. Mackenzie. *Anhydrous chlorides of some rare earths.* J. Inorg. Nucl. Chem. 32, 43 (1970).

19. Audrieth, L.F. and J. Kleinburg. *Non-aqueous solvents.* (J. Wiley & Sons, Inc., New York) 1958.

20. Heller, A. *Liquid lasers: preparative techniques for selenium oxychloride based solutions.* J. Am. Chem. Soc. 90, 3711 (1968).

21. Lamont, R.G., Watanabe, A. and J.G. Chambers. *A dry inert-gas glove box for the handling of hygroscopic and corrosive materials.* CRC Report No. 1244, (1973).

22. Dieke, G.H. and H.M. Crosswhite. *The spectra of the doubly and triply ionized rare earths.* Appl. Opt. 2, 675 (1963).

23. Lea, K.R., Leask, M.J.M. and W.P. Wolf. *The raising of angular momentum degeneracy of f-electron terms by cubic crystal fields.* J. Phys. Chem. Solids 23, 1381 (1962).

COMMUNICATIONS
CANADA